Experimental analysis of the effective thermal conductivity enhancement of PCM using finned tubes in high temperature bulk tanks

Antoni Gil[1,2], Gerard Peiró[1], Eduard Oró[1,3], Luisa F. Cabeza[1,*]

[1]GREiA Research Group, INSPIRES Research Centre, Universitat de Lleida, Pere de Cabrera s/n, 25001, Lleida, Spain

[2]Department of Mechanical Engineering, Massachusetts Institute of Technology, 77 Massachusetts Avenue, Cambridge, MA 02139, United States of America

[3]IREC, Jardins de les Dones de Negre 1, 2ª pl.08930 Sant Adrià de Besòs Barcelona, (Spain)

*Corresponding author: lcabeza@diei.udl.cat

Abstract

Solar cooling is a promising solution to overcome the high energy demand of buildings. Nevertheless, the time dependent nature of the solar source leads to the need of storage systems in order to better match the energy demand and supply. For this purpose, thermal energy storage was considered during last decades as the optimal solution at commercial scale. Latent thermal energy storage offers higher energy densities together with more constant outlet temperature than sensible heat storage, but the low thermal conductivities of PCMs represents the main drawback which limits its applicability. Several studies based on heat transfer enhancement techniques applied in latent thermal energy storage have already been performed. Specifically, the technique of adding fins in storage tanks, which is the most known and studied. However, there are few experimental studies at pilot plant scale focused on this technique and less on the analysis of the heat transfer enhancement through the parameter effective thermal conductivity. This paper presents an experimental study where this parameter is determined and compared using of two identical latent storage tanks, one with 196 transversal squared fins and another one without fins. In this case, hydroquinone was selected as PCM. A set of six experiments was performed at pilot plant of the University of Lleida (Spain), combining three different HTF flow rates and two temperature gradients between HTF inlet temperature and initial PCM temperature. Experimental results showed that the addition of fins can increase the effective thermal conductivity between 4.11% and 25.83% comparing the experiment with highest and lowest thermal power supplied to the PCM, respectively.

Keywords: effective thermal conductivity; phase change material; solar cooling; storage tank with fins; thermal energy storage

Nomenclature

A	Surface, m^2
D	Diameter, m
e	Distance between fins, m
h	Specific enthalpy, J/kg·K
HTF	Heat transfer fluid, -
k	Thermal conductivity, W/m·K
L	Average pipe length, m
LTES	Latent thermal energy storage, -
m	Mass, kg
N	Number of fins, -
PCM	Phase change material
$\dot{Q}$	Heat transfer rate, W
S	Shape factor, m
T	Temperature, ºC
TCES	Thermochemical energy storage
TES	Thermal energy storage
U	Global heat transfer coefficient, $W/m^2 \cdot K$
W	Distance between pipes, m
WF	With fins, -
WOF	Without fins, -

Greek symbols

η	Efficiency, -
θ	Mel fraction, -

Subscripts

cond	Conduction heat transfer
eff	Effective
eq	Equivalent
ext	External
f	Final
fin	Fins
i	Initial
in	Inlet
L	Liquid

out	Outlet
Tube	Tube
S	Solid

1. Introduction

Buildings represent one of the dominating energy-consumption sectors in the world. During the last decades the energy consumption for air-conditioning in the residential sector increased dramatically in these countries leading to a high demand on the available electric power based on the exploitation of fossil fuels, which causes green-house gases emissions. Solar cooling is a sustainable alternative to provide a source of industrial and residential cooling [1]-[3]. A wide variety of cooling techniques powered by solar collector-based thermally driven cycles have been developed and applied in the last decades [4].

Since solar energy is time dependent, the successful utilization of all these systems is a very degree dependent on the thermal energy storage (TES) systems used: integrating TES systems to solar cooling applications contributes to consumption reduction from the grid on demand peaks and hence, economic savings. A study about TES potential in buildings sector presented by Arce et al. [5] demonstrated that just in Spain TES systems may potentially help to save 140,883 GWh_{th} in domestic cooling applications.

Three types of TES systems may be basically applied in solar cooling applications: sensible heat (STES), latent heat (LTES), and thermochemical (TCES) [6],[7]. Concerning to the LTES systems, these are based on phase change materials (PCM), which allow storing larger quantity of energy per volume in comparison with STES systems. Moreover, PCM are already well known for constant working temperature for thermal storage applications. Nevertheless, PCM show generally low thermal conductivity even in the liquid phase (usually lower than 1 W/m·K) limiting the power during charging/discharging processes and definitely LTES systems applicability. For this reason, a research effort on heat transfer enhancement techniques in LTES has been done [8]. One the one hand, the heat transfer enhancement techniques are focused on enhancing the PCM by its combination with highly thermal conductive materials (graphite composites, metal foams composites, and nanomaterials). One of the studies focused on this topic was presented by Marin et al. [9], who studied experimentally and numerically the melting and solidification processes of pure paraffin (used as cold storage material) encapsulated in plate and a porous graphite matrix. This paper demonstrated that the graphite matrix with embedded PCM presented better results in terms of thermal conductivity improvement. Regarding on the use of metal foams, Zhang et al. [10] experimentally and numerically investigated the thermal enhancement of a eutectic mixture, $KNO_3/NaNO_3$, by combining it with copper and nickel metal foams. They observed an improvement during the discharging process in 28.8% and 19.3%, respectively. As mentioned previously, another technique focused on enhancing the thermal conductivity of PCM is the addition of highly conductive nanoparticles within a TES material. Shi et al. [11] and Yuan et al. [12],[13] showed an enhancement up to 60% in thermophysical properties in cementitious TES materials with SiO_2, MgO, and Cu nanoparticles in comparison with pure material.

One the other hand, the most known heat transfer technique is focused on enhancing the heat transfer between heat transfer fluid (HTF) and PCM by the addition of extended surfaces. A theoretical study was carried out by Tamme et al. [14] where the addition of fins of graphite was proposed in order to optimize the steam accumulators operating with salts as PCM. The results show a reduction of the number of pipes. Other numerical studies were carried out by Zhang and Faghri [15], Seeniraj et al. [16], Guo and Zhang [17], and Tiari et al. [18]. All these studies show significant improvements in the heat transfer rates between HTF and PCM depending on the geometry of the fins, their spacing, the tube diameter, the boundary conditions, and the thermal conductivity of the PCM selected. Tao et al. [19] numerically studied three geometrically different fins enhancement techniques (dimpled, cone-fined and helically-fined) in a LTES system. They show a reduction on the melting time of 19.9%, 26.9 %, and 30.7 %, respectively. This idea led other researchers to study the use secondary fins. For example Khaled [20] compared hairy fins to the more known rectangular fins. Similarly, secondary fins were used by Abujas et al. [21]. Both authors showed that the use of secondary fins results in a more homogeneous temperature in the PCM. Recently Dhaidan et al [22] reviewed the analytical computational, and experimental studies focused on the enhancement of the performance of PCM through the addition of high thermal conductivity fins. They also was found that the number of fins and fin length have stronger effects on the performance of the storage system than those caused by fin thickness and fin orientation. Moreover they highlighted that the conflict between enhancement of the effective thermal conductivity and simultaneous suppression of the buoyancy effect should be considered by the designer through selecting the optimum positions and orientation of the fins

In general, as observed from the available literature, heat transfer improvements by addition of fins in LTES systems have been widely demonstrated by several studies. But most of them are numerical or experimental at small scale. As stated by Rathgeber et al.[23], the behaviour of TES materials could be size-dependant. Hence, experimental studies at large scale are needed. However, few experimental studies focused on LTES systems at high temperature applications which demonstrate the applicability of adding fins at large scale can be found. This aspect is highlighted in two experimental studies done by Gil et al. [24],[25], who used two high temperature PCM tanks to be used in solar cooling, one with fins and the other one without fins. The PCM used was hydroquinone, with a melting temperature range of 167-173ºC. In first study [24] the authors calculated the average effectiveness of both tanks as a function of the tank design parameters. Results showed that for the storage tank without fins the relation matched with that previously published by other authors, while a new relationship was defined for tanks with fins. In the second study [25], both tanks were used to experimentally determine the influence of the addition of fins in the PCM melting and solidification time. The authors found that when using fins in a PCM tank, not only the time response has to be taken into account, but also the power.

Therefore, experimental studies are needed to determine the variation of the effective thermal conductivity of PCM by the use of fins in high temperature LTES tanks. Francis et al [26] proposed a mathematical formulation to calculate thermal effective conductivity in Yucca Mountain, Nevada, drift enclosures for radioactive waste applications. This formulation allowed modelling natural convection heat transfer as a conduction-only model.

In the present study, an adapted mathematical formulation from the proposed by Francis et al. [26] was used in order to study experimentally the effective thermal conductivity of a high temperature PCM using the previously mentioned LTES tanks. The results presented in this paper extends the information shown in previous mentioned studies [24],[25].

2. Materials and methodology

2.1. Phase change material and experimental set-up

The material selected to be used as PCM was hydroquinone since its melting temperature range is within the range required for solar cooling applications (150 ºC to 200 ºC) and the phase change enthalpy is higher than the minimum value required, fixed on 150 kJ/kg. The phase change temperature range and the latent heat of fusion of hydroquinone were measured by DSC analysis which was presented in a previous work published by Gil et al. [27]. The average value of main thermophysical properties of hydroquinone within its melting range are shown in **Table 1**.

Table 1. Average value of thermophysical properties of hydroquinone within its melting range [27]-[29]

Properties	Units	Values
Melting temperature range	[ºC]	168-173
Melting enthalpy	[kJ/kg]K]	205.8
Density	[kg/m^3]	1180.1
Thermal conductivity	[W/m·K]	0.1
Dynamic viscosity	[mPa·s]	0.97

The experimental facility used in this study was built in 2008 at University of Lleida to test different materials, systems, instrumentation and operational strategies for high temperature TES applications such as solar cooling and concentrated solar power. An accurately description of its main components was provided by Cabeza et al. [30]. Figure 1 shows a scheme of the pilot plant.

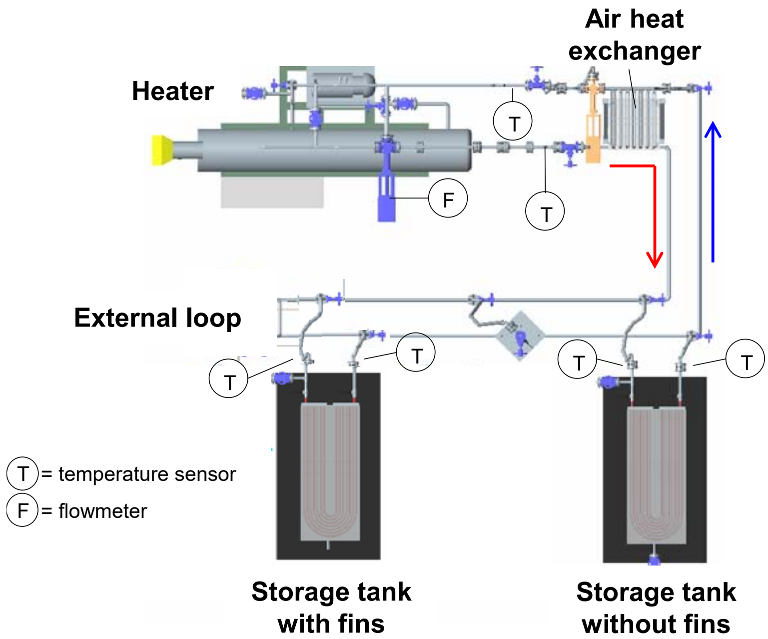

Figure 1. Scheme of the pilot plant available at the University of Lleida during the charging process

In order to perform the experiments, two LTES tanks based on shell and tubes design available in pilot plant of University of Lleida were used (Figure 2a).

In these tanks, the PCM was located in the housing of the shell part and the HTF circulates inside the bundle of tubes, which was integrated for 49 tubes distributed in square pitch. The tubes were bended in U shape and they were connected in each side to collectors which distribute the HTF equally in all the tubes. One of the units incorporated transversal fins of 0.5 mm of thickness assembled in the tubes bundle (Figure 2b). Table 2 shows the main characteristics of both storage tanks used.

Table 2. Storage tank dimensions and parameters

	PCM tank without fins	PCM tank with fins
Tank width [m]	0.527	0.527
Tank height [m]	0.273	0.273
Tank depth [m]	1.273	1.273
Material of tank	Stainless steel 304L	
Number of HTF tubes [-]	49	49
Pipe outlet diameter [mm]	17.2	17.2
HTF pipes average length [m]	2.408	2.408
Heat transfer surface [m^2]	6.568	26.688
Number of fins [-]	-	196
Dimensions of fins [m]	-	0.25 x 0.25
Thickness of fins [mm]	-	0.5
Distance between fins [mm]	-	10
Material of fins	-	Stainless steel 304L
PCM mass [kg]	170	155
Latent energy storage capacity [kJ]	39,984	36,456
Latent energy storage capacity [kWh]	11.10	10.12

A total of 15 temperature sensors were installed along each tank for an accurate analysis of the PCM thermal behaviour. The sensors were installed between the HTF tubes bundle ($T_{PCM.1}$ to $T_{PCM.15}$), as it may be seen in Figure 2b. These sensors were distributed, along the length of the storage tank in three heights at 22 mm, 117 mm and 181 mm from the bottom of the tank and with three different positions in the horizontal plane. The sensors at the bottom, middle and top zone were located at 35 mm, 114 mm, and 194 mm respect to the wall of the tank (Figure 2b). Two more sensors were installed in the inlet and outlet (T_{HTFin} and T_{HTFout}) of each tank to measure the HTF temperature. All the temperature sensors were Pt-100 with an accuracy of 2%.

To minimize the heat losses from the storage tank to the surroundings, 24 cm of rock wool were installed on the lateral walls and on the top of the storage tanks while 45 cm of Foamglass® were installed at the bottom.

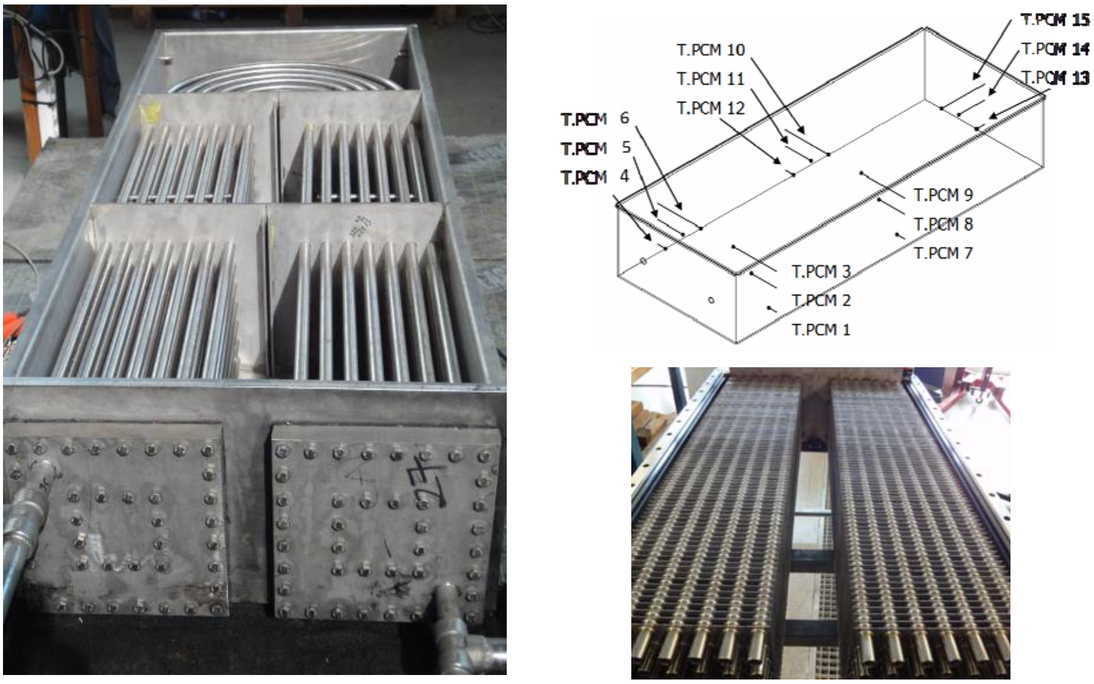

(a) (b)

Figure 2. Storage tank built. (a) U shape tubes bundle and (b) Position of the temperature sensors and finned bundle

2.2. Experimental procedure

To evaluate the effective thermal conductivity of the PCM, 12 experiments were performed: six experiments were performed with the storage tank without fins and six more using the storage tank with fins. Experiments consisted of several charging processes performed on two different temperature gradients between HTF inlet temperature (T_{HTFin}) and initial PCM temperature (T_{PCMi}): 145-187 ºC and 130-200 ºC, considering a tolerance of ±2 ºC. Before the experiment started, a warm-up period was defined to achieve initial PCM temperature (T_{PCMi}). Then, the HTF was heated up outside the tank until the desired HTF inlet temperature (T_{HTFin}) was reached and introduced into the storage tank, starting the charging process. In each experiment, the duration of the charging was 8 hours. The volumetric flow rate of the HTF was varied between 1.4 m^3/h and 3.0 m^3/h, as it may be seen in Table 3. It should be pointed out the HTF flow rate control experienced small fluctuations because of PID control system and a tolerance of ±0.05 m^3/h had to be considered on each. In addition, the used LTES tanks were designed according to the specifications given by real absorption chiller located at University of Seville.

Furthermore were tested under different operational conditions (Table 3) within the operational range allowed by the mentioned absorption chiller. For this reason the result showed in following sections will be only valid for the used experimental set-up.

Table 3. Nominal volumetric flow, nominal temperature gradient and Reynolds during the different charging processes performed in each experiment

Without fins (WOF) /with fins (WF)	Nominal temperature gradient (T_{PCMi}-T_{HTFin}) [ºC]	Nominal volumetric flow rate [m^3/h]	Reynolds [-]
WOF1	145-187	1.4	1633
WF1			1646
WOF2		2.2	2566
WF2			2564
WOF3		3.0	3482
WF3			3447
WOF4	130-200	1.4	1775
WF4			1757
WOF5		2.2	2792
WF5			2725
WOF6		3.0	3785
WF6			3602

2.3. Mathematical formulation

Effective thermal conductivity is a parameter widely used to model natural convection as conduction-only model. Francis et al. [26] defined the effective thermal conductivity as an enhanced thermal conductivity by means of a parameter, called equivalent thermal conductivity, which is the ratio between the total heat transfer (considering convection and conduction heat transfer) and the conduction heat transfer.

The mathematical formulation used in the current study and presented in this section was adapted from the formulation proposed by Francis et al. [26] and was used to consider the effect of the natural convection on the side of the liquid phase of PCM of both tanks tested during the melting process (Eq.1 and Eq.2):

$$k_{eff} = k_{eq} \cdot k_{PCM} \quad (1)$$

$$k_{eq} = \frac{\dot{Q}_{PCM}}{(\dot{Q}_{PCM})_{cond}} \quad (2)$$

where $\dot{Q}_{PCM}$ corresponds to the thermal power stored by the PCM during the melting process taking into account the convection and conduction heat transfer mechanisms. This parameter was calculated considering the increase of specific enthalpy of hydroquinone between the beginning and the end of the melting process applied to squared control volume. This control volume was defined taking into account only one tube of the internal core of the tubes bundle (Figure 3) to reduce the influence of heat losses and to obtain reference temperature behaviour of the PCM. For this reason, even though the PCM temperature was measured in different points of the tank (Figure 2b), sensors placed in the middle of the tube bundle and at half of the height of the tank (T.PCM 8 and T.PCM 11) were defined as PCM temperature reference of control volume. Moreover, to evaluate solely the PCM latent heat behaviour during the charging, the evaluation process was focused only within the melting temperature range (167-173 ºC):

$$\dot{Q}_{PCM} = m_{PCM} \cdot \frac{h_f - h_i}{t_f - t_i} \quad (3)$$

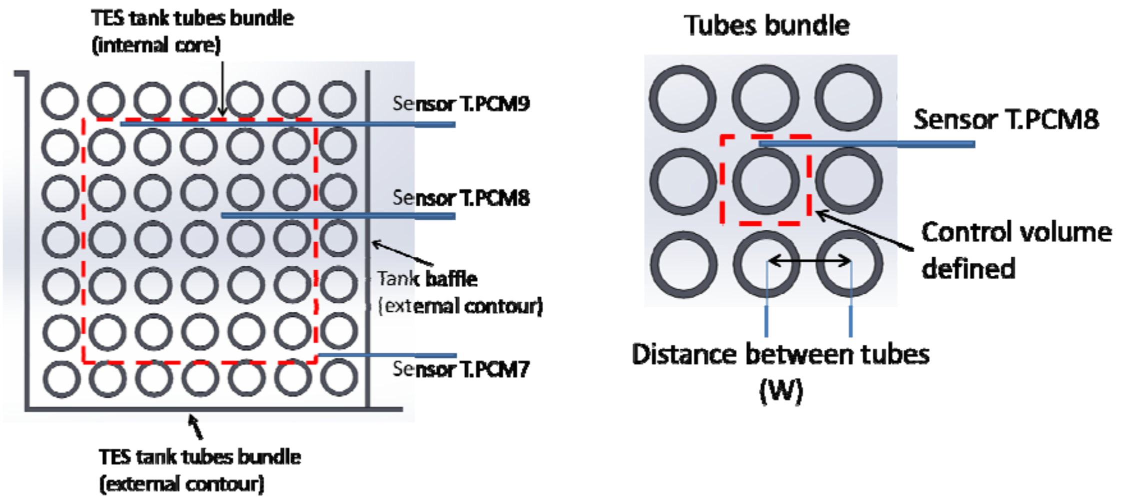

(a) (b)

Figure 3. External contour and internal core of the tubes bundle, including position of temperature sensor T.PCM8 and (b) Control volume defined to calculate the PCM effective conductivity

On the other hand, $(\dot{Q}_{PCM})_{cond}$ is the thermal power stored by control volume of PCM taking into account only the conduction heat transfer mechanism.

To calculate this parameter, the two dimensional conduction problem applied to one circular pipe model proposed by Peiró et al. [31] was considered for tank without fins (Eq.4).

$$\left(\dot{Q}_{PCM}\right)_{cond.wof} = k_{PCM} \cdot S \cdot \left(T_{Tube} - T_{PCM}\right) \quad (4)$$

where S is a shape factor (Eq.5) for the presented 2-D conduction problem consisting of circular cylinder of length L centred in a square solid of width W and equal length (Figure 4) [32].

$$S = \frac{2 \cdot \pi \cdot L}{\ln\left(1.08 \cdot \frac{W}{D_{ext}}\right)} \quad (5)$$

Table 4 shows the values of parameters necessary to calculate the shape factor.

Table 4. Storage tank parameters to calculate the shape factor

Parameter	Value	Units
L	2480	mm
W	31	mm
D_{ext}	17.2	mm

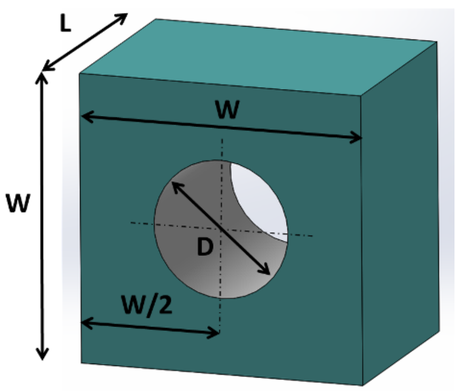

Figure 4. Shape factor selected for the storage tanks and parameters to characterize it [32]

For tank with fins, the total conduction heat transfer rate was calculated as the addition of conduction heat transfer rates of both the exposed surface of the HTF tube and the fins. The conduction heat transfer rate of the exposed surface of the HTF tube was obtained as in tank without fins (Eq.4). However for the fins was calculated taking into account its maximum possible conduction heat transfer rate and its thermal efficiency (Eq.6). Notice that the maximum possible conduction heat transfer rate would result if the entire fin surface was maintained at temperature of he exposed surface of the HTF tube (T_{Tube}).

$$(\dot{Q}_{PCM})_{cond.wf} = k_{PCM} \cdot S \cdot (T_{Tube} - T_{PCM}) + \eta_{fin} \cdot N \cdot k_{PCM} \cdot A_{fin} \cdot \frac{(T_{Tube} - T_{PCM})}{\frac{e}{2}} \quad (6)$$

Figure 5 was used to obtain the thermal efficiency of single fin η_{fin}, considering circular fin with the same area as squared fin used in this study. Moreover parameter $\frac{2 \cdot k_{PCM}}{e}$ was used instead of natural convection heat transfer coefficient. From Figure 5 an efficiency of 82% was obtained.

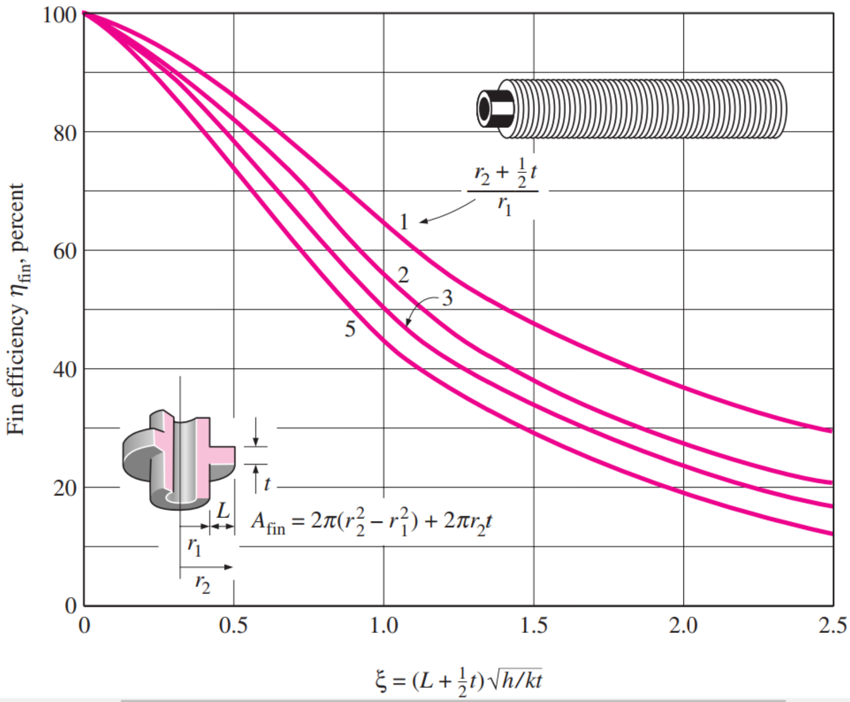

Figure 5. Efficiency of circular fin of length L and constant thickness t [33]

The following assumptions during the melting process were introduced to simplify the analysis:

- Small thermal gradient between HTF inlet and outlet.
- Constant wall temperature along the tubes, which is defined as the mean temperature between HTF inlet and outlet.
- Variable thermophysical properties with the temperature.
- The phase change temperature was the mean of the maximum and minimum temperatures of the melting range (167 ºC-173 ºC).

- The melting front progress was considered in radial direction and concentric to the pipe.

Finally, in order to evaluate the performance of the melting process in both tanks, the melt fraction of PCM was calculated. The melt fraction of the PCM can be calculated based on the lever rule between the solid and liquid temperatures during the charging process as Eq.7 shows. The melt fraction of the PCM takes the value of 0 at the beginning of melting process when PCM is completely solid, and when it reaches the value of 1 it means that the PCM is completely melted.

$$\theta = \frac{T_{PCM} - T_S}{T_L - T_S} \tag{7}$$

3. Results and discussion

Figure 6 shows the melting process of the PCM during experiments with a temperature range between 145-187 ºC and a flow rates of 1.4, 2.2 and 3 m^3/h, for each tank configuration (with and without fins). And Figure 7 shows the same results for temperature range between 130-200 ºC. In these figures, HTF inlet temperature (HTF in) is plotted in red, while HTF outlet temperature (HTF out) is plotted in blue. Moreover, in order to validate the mathematical formulation presented in previous section, T.PCM 8 and T.PCM 11 are plotted and compared. The PCM melting range is represented by shaded area.

From the temperature profiles, is observed when the HTF flow rate is higher the PCM charging process in both tanks develops faster due to the high power transferred by HTF to the PCM. And on the other hand, as expected, the melting process starts earlier and is shorter in the experiments in the tank with fins on the tubes bundle of the storage tank. Moreover, as can be seen in Figure 7 the difference observed in melting time of PCM between both tanks is lower.

Notice that T.PCM 8 and T.PCM 11 show practically the same behaviour in all experiments performed with both tanks. This fact validates the mathematical formulation used to obtain the effective thermal conductivity of the PCM and allows using both T.PCM 8 and T.PCM 11 as reference control volume PCM temperature.

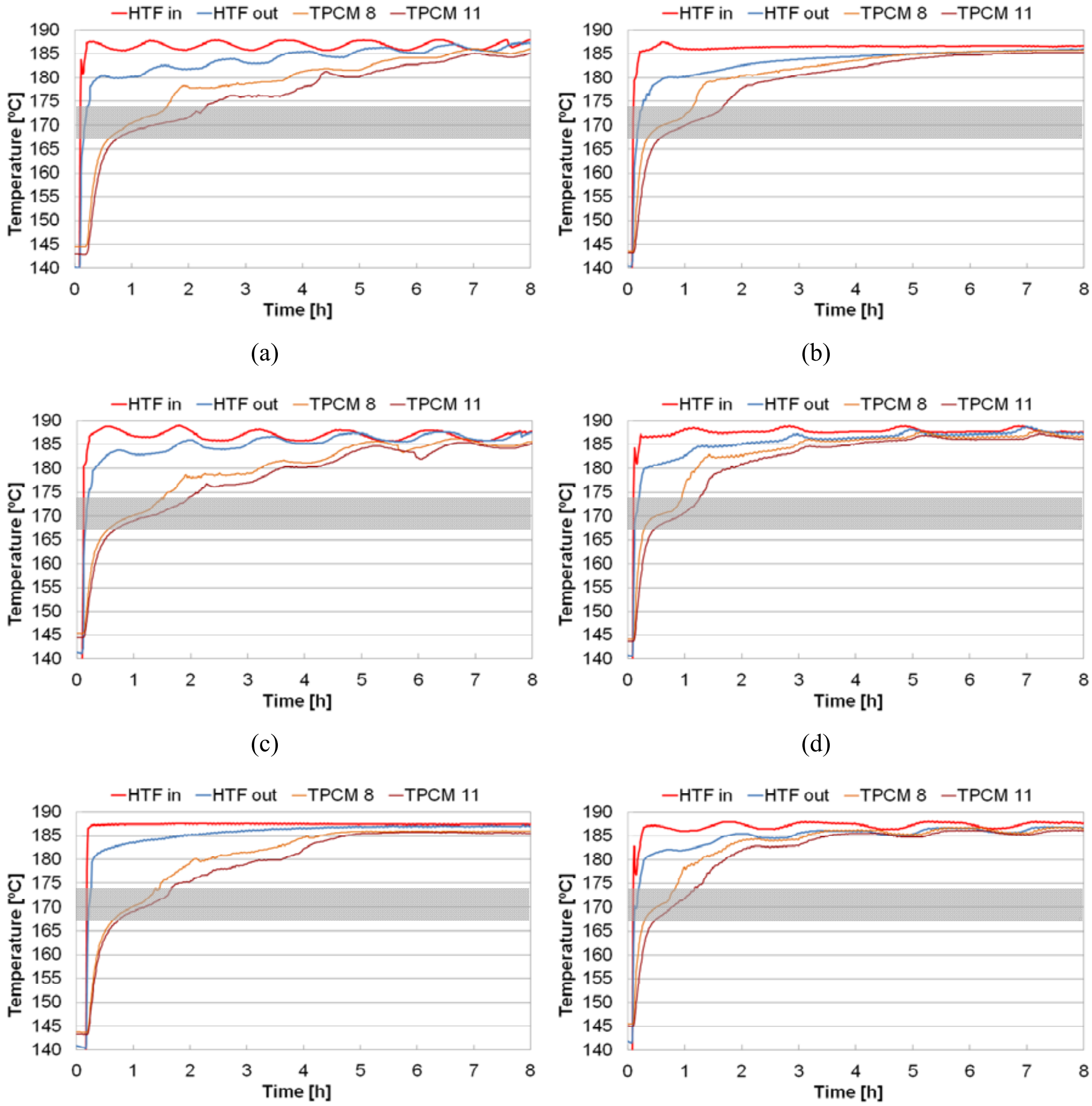

(a) (b) (c) (d) (e) (f)

Figure 6. Storage tanks (with and without fins) melting process for experiment with a temperature range between 145-187 ºC. (a) No fins with flow rate of 1.4 m^3/h (WOF1), (b) With fins with flow rate of 1.4 m^3/h (WF1), (c) No fins with flow rate of 2.2 m^3/h (WOF2), (d) With fins with flow rate of 2.4 m^3/h (WF2), (e) No fins with flow rate of 3 m^3/h (WOF3), (f) With fins with flow rate of 3 m^3/h (WF3)

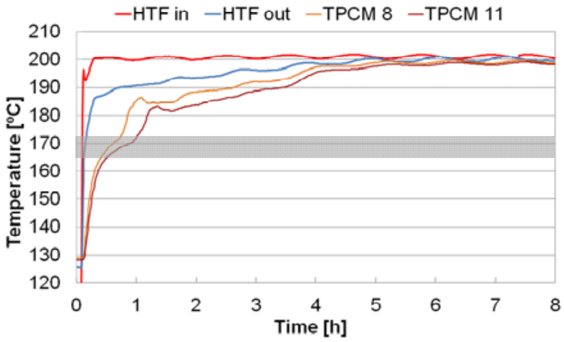

(a)

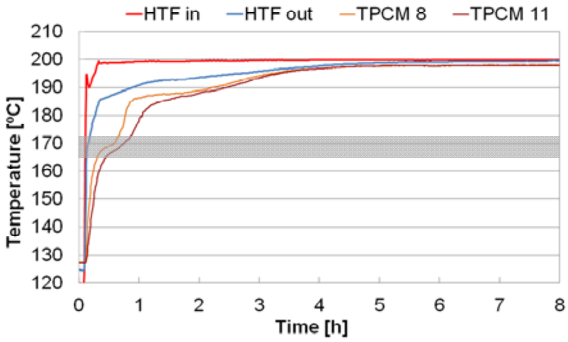

(b)

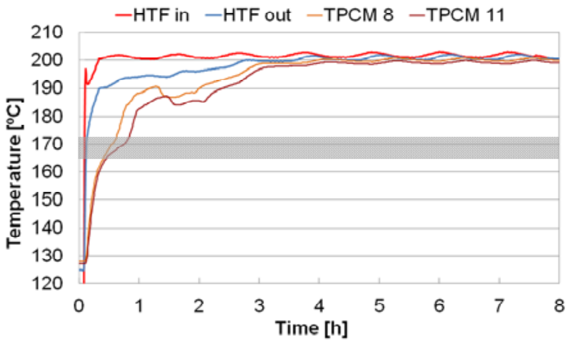

(c)

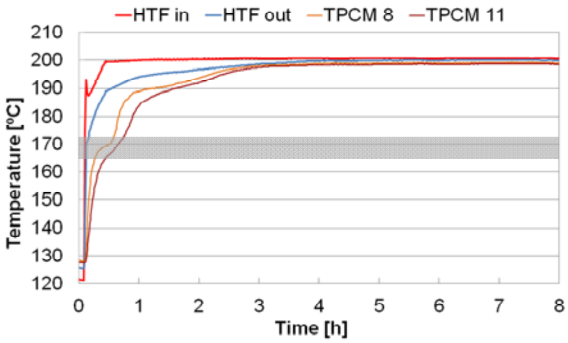

(d)

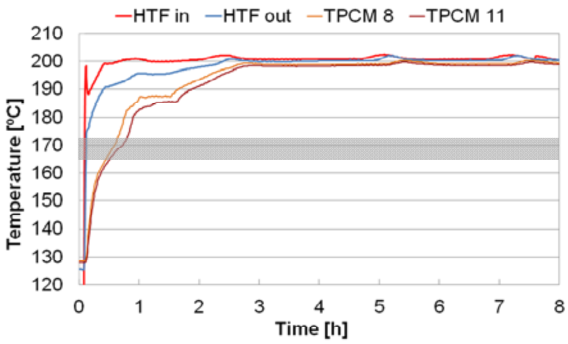

(e)

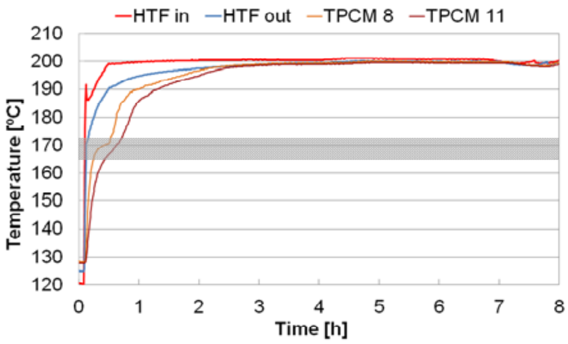

(f)

Figure 7. Storage tanks (with and without fins) melting process for experiment with a temperature range between 130-200 ºC. (a) No fins with flow rate of 1.4 m^3/h (WOF4), (b) With fins with flow rate of 1.4 m^3/h (WF4), (c) No fins with flow rate of 2.2 m^3/h (WOF5), (d) With fins with flow rate of 2.2 m^3/h (WF5), (e) No fins with flow rate of 3 m^3/h (WOF6), (f) With fins with flow rate of 3 m^3/h (WF6)

Figure 8a shows the melt fraction of the PCM during the charging process of both tanks of the tests with a thermal gradient between 145-187 ºC. Figure 8b shows the melt fraction of the PCM during the charging process of both tanks of the tests with a thermal gradient between 130-200 ºC. In Figure 8 the solid lines show the melt fraction of the tests performed with tank without fins and dotted lines the tests performed with tank with fins.

As it may be seen, the time of melting is shorter for the TES tank with fins under the same flow and temperature gradient. At lower values of power supplied to PCM, the melt fraction of PCM increases faster in tests performed with tanks with fins (Figure 8a), especially in tests WOF1/WF1 to WOF3/WF3. However at higher thermal power supplied to PCM (Figure 8b) the melt fraction of PCM shows practically the same behaviour in both tanks especially in tests WOF5/WF5 and WOF6/WF6.

Hence, these facts indicate that the addition of transversal fins to the tubes bundle of a storage tank helps to enhance the effective conductivity of the PCM. The reduction of melting time is evident for low power values and decreases for high values. The reason lies on the fact that under a laminar flow regime, the heat transfer coefficient and the limiting thermal resistance is on the PCM side, which is reduced with the addition of fins due to the increase of heat transfer surface between HTF and PCM. On the contrary, at higher power, when the HTF flow regime is intermediate or turbulent and thermal gradient between HTF and PCM is higher, the enhancement of using fins is not as important as the enhancement of increasing the convective heat transfer coefficient on the HTF side.

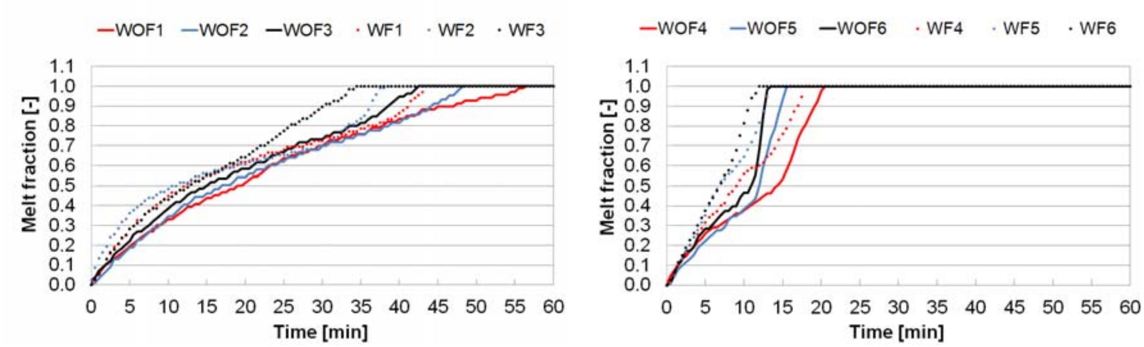

(a) (b)

Figure 8. Melt fraction profile. (a) Tests with both tanks at temperature range between 145-187 ºC and (b) Tests with both tanks at temperature range between 130-200 ºC

Table 5 shows, the effective thermal conductivity for both storage tanks and for each experiment performed. As it was explained, the effective thermal conductivity is a parameter used to model the effect of natural convection of PCM as conduction-only model. Since the natural convection depends indirectly on the power supplied to the PCM, the effective thermal conductivity is not a constant value. The increase of the effective thermal conductivity due to the inclusion of fins varies between 4% and 26%, depending on the flow rate and temperature gradient used in the charging process.

Table 5. PCM effective thermal conductivity obtained for each experiment performed

Experiment Without fins (WOF)/With fins (WF)	Effective thermal conductivity [W/m·K]		
	Without fins (WOF)/	With fins (WF)	%
WOF1/WF1	0.45	0.57	25.83
WOF2/WF2	0.50	0.59	18.47
WOF3/WF3	0.55	0.63	12.3
WOF4/WF4	0.61	0.67	11.40
WOF5/WF5	0.66	0.69	4.41
WOF6/WF6	0.71	0.73	4.11

4. Conclusions

In the present paper the authors studied experimentally the effect of adding fins in LTES systems from the study of effective thermal conductivity of PCM under different power ratios supplied to the PCM. Consequently, two TES tanks based on a shell-and-tubes heat exchanger concept were used. These were built at the University of Lleida, one of them including 196 squared fins. A total of six experiments were carried out for each storage tank, varying the flow rate from 1.4 to 3.0 m^3/h and the heat transfer fluid (HTF) working temperature gradient, 42 ºC and 70 ºC.

Effective thermal conductivity of PCM was defined as an enhanced thermal conductivity calculated through the ratio between total heat transfer of PCM and conduction heat transfer applied to one control volume consisted of one tube of the core bundle was defined for each tank.

The results obtained showed that the fins assembled on the storage tank tubes bundle helped to enhance the PCM effective thermal conductivity, showing values from 0.57 W/m·K up to 0.73 W/m·K. Comparing with the storage tank without fins, this values represent an improvement on the effective thermal conductivity between 4.11% comparing the experiments performed with the highest thermal power supplied to PCM of each tank, and 25.83% comparing the experiment performed with lowest thermal power. The same behaviour was observed in the study of melt fraction for all experiments. The time reduction and the melt fraction enhancement between the tank with and without fins is evident lower values of thermal power supplied to PCM, while in the experiments with highest thermal power supplied to PCM the temperature gradient between the PCM and the HTF is large enough to reduce the fins effect.

These results contribute to demonstrate that the use of fins in a storage tank helps to improve the PCM effective thermal conductivity during the melting process and could be a powerful tool for partial charging or discharging processes. Moreover, the use of the effective thermal conductivity demonstrated to be decisive in order to easily and experimentally evaluate the improvement of the fins on the heat exchange process in a TES system using PCMs.

Acknowledgements

The work was partially funded by the Spanish government (ULLE10-4E-1305 and ENE2015-64117-C5-1-R (MINECO/FEDER)). The authors would like to thank the Catalan Government for the quality accreditation given to their research group GREA (2017 SGR 1537). GREA is certified agent TECNIO in the category of technology developers from the Government of Catalonia.

References

[1] H.M. Henning, Solar-assisted air-conditioning in buildings. A handbook for planners, Wien: ed. Springer; 2004.

[2] M.S. Fernandes, G.J.V.N. Brites, J.J. Costa, A.R. Gaspar, V.A.F. Costa, Review and future trends of solar adsorption refrigeration systems, Renew. Sustain. Energy Rev. 39 (2014) 102-123.

[3] G.J.V.N. Brites, J.J. Costa, V.A.F. Costa, Influence of the design parameters on the overall performance of a solar adsorption refrigerator, Renew. Energ. 86 (2016) 238-250.

[4] L.A. Chidambaran, A.S. Ramana, G. Kamaraj, R. Verlaj, Review of solar cooling methods and thermal storage options, Renew. Sustain. Energy Rev. 15 (2011) 3220-3228.

.

[5] P. Arce, M. Medrano, A. Gil, E. Oró, L.F. Cabeza, Overview of thermal energy storage (TES) potential energy savings and climate change mitigation in Spain and Europe, Appl. Energy 88 (2011) 2764-2774.

[6] L.F. Cabeza, C. Solé, A. Castell, E. Oró, A. Gil, Review of Solar Thermal Storage Techniques and Associated Heat Transfer Technologies, Proceedings of the IEEE 100 (2011) 525-538.

[7] L. F. Cabeza, Advances in Thermal Energy Storage Systems: Methods and Applications, 2014, 1-592.

[8] J. Gasia, L. Miró, L.F. Cabeza, Materials and system requirements of high temperature thermal energy storage systems: A review. Part 2: Thermal conductivity enhancement techniques, Renew. Sustain. Energy Rev. 60 (2016) 1584-1601.

[9] J.M. Marin, B. Zalba, L.F. Cabeza, H. Mehling, Improvement of a thermal energy storage using plates with paraffin-graphite composite, Int. J. Heat Mass Tran. 48 (2005) 2561-2570.

[10] P. Zhang, X. Xiao, Z.N. Meng, M. Li, Heat transfer characteristics of a molten-salt thermal energy storage unit with and without heat transfer enhancement, Appl. Energy 137 (2015) 758–72.

[11] Y. Shi, H.W. Yuan, Z.Z. Xu, C.H. Lu, Y.R. Ni, Y. Dong, Thermal and mechanical properties of aluminate cementitious functional materials enriched with nano-SiO_2 for thermal energy storage, Adv. Mater. Res. 887-888 (2014) 77-80.

[12] H. Yuan, Y. Shi, Z. Xu, C. Lu, Y. Ni, X. Lan, Effect of nano-MgO on thermal and mechanical properties of aluminate cement composite thermal energy storage materials Ceram. Int. 40 (2014) 4811–4817.

[13] H. Yuan, Y. Shi, C. Lu, Z. Xu, Y. Ni, X. Lan, Enhanced performance of high temperature aluminate cementitious materials incorporated with Cu powders for thermal energy storage, Cem. Concr. Compos. 55 (2015)139–44.

[14] R. Tamme, T. Bauer, J. Buschle, D. Laing, H. Müller-Steinhagen, W.D. Steinmann, Latent heat storage above 120 ºC for applications in the industrial process heat sector and solar power generation, Int. J. Energ. Res. 32 (2008) 264-271.

[15] Y. Zhang, A. Faghri, Heat transfer enhancement in latent heat thermal energy storage system by using the internally finned tube, Int. J. Heat Mass Tran. 39 (1996) 3165-3173.

[16] R.V. Seeniraj, R. Velraj, N.L. Narasimhan, Thermal analysis of a finned tube LHTS module for a solar dynamic power system, Heat Mass Transfer 38 (2002) 409-417.

[17] C. Guo, W. Zhang, Numerical simulation and parametric study on new type of high temperature latent heat thermal energy storage system, Energ. Convers. Manage. 49 (2008) 919-927.

[18] S. Tiari, S. Qiu, M. Mahdavi, Numerical study of finned heat pipe-assisted thermal energy storage system with high temperature phase change material, Energ. Convers. Manage. 89 (2015) 833-842.

[19] Y.B. Tao, Y.L. He, Z.G. Qu, Numerical study on performance of molten salt phase change thermal energy storage system with enhanced tubes, Sol. Energy 86 (2012) 1155-1163.

[20] A.-R.A. Khaled, Heat transfer enhancement in hairy fin systems, Appl. Therm. Eng. 27 (2007) 250-257.

[21] C.R. Abujas, A. Jové, C. Prieto, M Gallas, L.F. Cabeza, Performance comparison of a group of thermal conductivity enhancement methodology in phase change material for thermal storage application, Renew. Energy 97 (2016) 434-443.

[22] N.S. Dhaidan, J.M. Khodadadi, Improved performance of latent heat energy storage systems utilizing high thermal conductivity fins: A review, J. Renew. Sustain. Ener. 9 (2017) 034103.
[23] C. Rathgeber, L. Miro, L.F. Cabeza, S. Hieber, Measurement of enthalpy curves of phase change materials via DSC and T-History. When both methods needed to estimate the behaviour of the bulk materials in applications, Thermochim. Acta. 596 (2014) 79–88.
[24] A. Gil, E. Oró, A. Castell, L.F. Cabeza, Experimental analysis of the effectiveness of a high temperature thermal storage tank for solar cooling applications, Appl. Therm. Eng. 54 (2013) 521-527.
[25] A Gil, E. Oró, L. Miró, G. Peiró, A. Ruiz, J.M Salmerón, L.F. Cabeza, Experimental analysis of hydroquinone used as phase change material (PCM) to be applied in solar cooling refrigeration, Int. J. Refrig. 39 (2014) 95-103.
[26] N.D. Jr. Francis, M.T. Itamura, S.W. Webb, D.L. James, CFD calculation of internal natural convection in the annulus between horitzontal concentric cylinders, SAND2002-3132 (2002), Albuquerqur, Newmexico: Sandia National Laboratories.
[27] A. Gil, E.Oró, G. Peiró, S. Álvarez, L.F. Cabeza, Material selection and testing for thermal energy storage in solar cooling, Renew. Energy 57 (2013) 366-371.
[28] C.L. Yaws, Thermophysical Properties of Chemicals and Hydrocarbons, 2nd Edition, Elsevier, The Boulevard, Langford Lane, Kidlington, Oxford, UK, 2014.
[29] C.L. Yaws, Transport Properties of Chemicals and Hydrocarbons, 2nd Edition, Elsevier, The Boulevard, Langford Lane, Kidlington, Oxford, UK, 2014.
[30] L.F. Cabeza, C. Prieto, L. Miró, J. Gasia, G. Peiró, Design and start-up of two pilot plants for Molten Salts Storage Testing, ASME 10th International Conference on Energy Sustainability, collocated with the ASME Power Conference and the ASME 14th International Conference on Fuel Cell Science, Engineering and Technology. Volume 1 (2016) Article number 59268.
[31] G. Peiró, J. Gasia, L. Miró, L.F. Cabeza, Experimental evaluation at pilot plant scale of multiple PCMs (cascaded) vs. single PCM configuration for thermal energy storage, Renew. Energ. 83 (2015) 729-736.
[32] G. Nellis, S. Klein, Heat transfer, first ed., Cambridge University Press, New York, 2009.
[33] K. A. Gardner, Efficiency of Extended Surfaces, Trans. ASME 67 (1945) 621–31.